PHYSICAL REVIEW B **80**, 060402(R) (2009)

Direct measurement of nonlinear ferromagnetic damping via the intrinsic foldover effect

Y. S. Gui, A. Wirthmann, N. Mecking, and C.-M. Hu*
Department of Physics and Astronomy, University of Manitoba, Winnipeg, Manitoba, Canada R3T 2N2
(Received 19 June 2009; published 27 August 2009)

An approach to measure precisely nonlinear ferromagnetic damping is demonstrated by using spin dynamos in combination with sensitive electrical probing techniques. The directly measured intrinsic foldover effect unravels a 50-year-old mystery of ferromagnetic metals. Pivotal importance of nonlinear ferromagnetic damping is uncovered via its distinct dependence on the frequency, amplitude, and initial conditions. The experimental results are in excellent agreement with a nonlinear oscillator model, which revises the pioneer work of Anderson and Suhl for nonlinear magnetization dynamics.

DOI: 10.1103/PhysRevB.80.060402 PACS number(s): 76.50.+g, 42.65.−k, 75.40.Gb

Nonlinear dynamics differ distinctly from linear response. For example, introducing a nonlinear restoring force into Galileo's pendulum[1] breaks the isochronism of harmonic oscillators and causes effects such as amplitude-dependent resonance frequency, foldover and bistability.[2] These nonlinear fingerprints are ubiquitous in nature, as found in mechanical[2] and magnetic[3,4] systems. Demanding technological issues such as microwave-assisted switching[5] and spin-torque nano-oscillators[6] require a clear grasp of nonlinear magnetization dynamics. Yet, the long-standing significant challenge in making quantitative measurements of nonlinear ferromagnetic dissipation has hampered understanding.

For over half a century, the foundation of ferromagnetic dissipation[7] has been built on the Gilbert damping model.[8] Based on the linearization of the Landau-Lifshitz equation, the intrinsic Gilbert damping constant α is commonly determined from the linewidth ΔH_0 of ferromagnetic resonance (FMR),[7] via the well-known relation

$$\Delta H_0 = \Delta H_i + \alpha\omega/\gamma, \tag{1}$$

where ΔH_i describes the nonintrinsic magnetic damping induced by inhomogeneities,[9] ω is the microwave frequency and γ is the gyromagnetic ratio. Equation (1) has been experimentally verified in the linear regime at sufficiently small magnetization precession angles θ. A recent theoretical breakthrough has elucidated the intrinsic nonlinear dissipation in ferromagnetic metals.[10] It leads to the open question of whether the standard Gilbert model is adequate in the nonlinear regime,[11] and it motivates us to develop an experimental approach to measure precisely nonlinear ferromagnetic dissipation in metals by utilizing spin dynamos.[12]

Our primary finding is that for θ above a few degrees, Eq. (1) is replaced by

$$\Delta H = \Delta H_i + \alpha\omega/\gamma + \beta M_0\theta^2, \tag{2}$$

which is dominated by the third term caused by nonlinear damping. Here M_0 is the saturation magnetization, β is a dimensionless but frequency-dependent damping constant describing nonlinear ferromagnetic dissipation. Equation (2) is established by studying FMR of Py microstrips. It fundamentally changes the picture of ferromagnetic dissipation in its frequency and amplitude dependences, which reveals the reason why foldover and bistability effects were not observed in any ferromagnetic metals previously, despite the pioneer work of Anderson and Suhl[3] which predicted such nonlinear fingerprints more than 50 years ago.[13]

To highlight the general features of nonlinear dynamics, we begin with a simple model of a classical oscillator $\ddot{x} = g(x,\dot{x})$ with mass $m=1$ under a general force $g(x,\dot{x})$. To the lowest approximation with only the linear restoring force $g(x)=-\omega_0^2 x$, this equation describes Galileo's pendulum [Fig. 1(a)], where ω_0 is the eigenfrequency of the free oscillation. Introducing the linear frictional force $-2\lambda\dot{x}$ into $g(x,\dot{x})$ requires a periodic external driving force $f\cos\omega t$ to compensate energy dissipation. Linear FMR [Fig. 1(h)] driven by a RF magnetic field $h\cos\omega t$ is similar to such a forced oscillation.

A nonlinear restoring force such as a term proportional to x^3 in $g(x,\dot{x})$ breaks the isochronism. As shown by Landau and Lifshitz,[2] when f is sufficiently small, the square of the resonant amplitude, a^2, as a function of the driving frequency ω shows a Lorentzian line shape centered at ω_0 with a linewidth $\Delta\omega\approx\lambda$ [Fig. 1(b)]. As f increases, the response becomes asymmetric and the maximum shifts away from ω_0 by an amount that is proportional to a^2. When f reaches a threshold value, f_{th}, the amplitude a has a threefold degenerate value near its maximum [Fig. 1(c)]. Foldover appears at $f>f_{th}$: depending on the history of sweeping ω, two abrupt

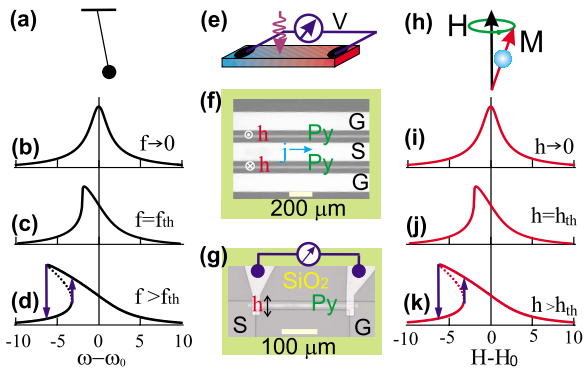

FIG. 1. (Color online) (a) Galileo's pendulum with the calculated amplitude a, as a function of $\omega-\omega_0$ at (b) $f=0.01f_{th}$, (c) $f=f_{th}$, and (d) $f=2f_{th}$. (e) Measurement scheme for photovoltage experiment. Top view micrograph of (f) sample I and (g) sample II selected from the first and second generation spin dynamos, respectively. (h) FMR with the calculated cone angle, θ, as a function of $H-H_0$ at (i) $h=0.01h_{th}$, (j) $h=h_{th}$, and (k) $h=2h_{th}$.

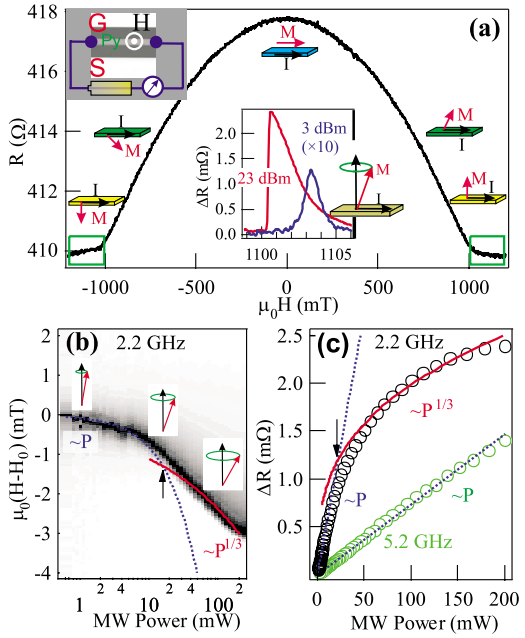

FIG. 2. (Color online) (a) Magnetoresistance (main panel) and photoresistance (bottom inset) which detect AMR and FMR, respectively. The magnetic field H is applied perpendicular to the Py strip (top inset). (b) Mappings of the power dependence of FMR detected by the photoresistance measurements. (c) ΔR as a function of the microwave power measured at 2.2 and 5.2 GHz. The dotted lines in (b) and (c) are calculated based on the relation $\theta^2 \propto P$, the solid lines are based on $\theta^2 \propto P^{1/3}$. The arrows in (b) and (c) mark a threshold power of $P_{th} \approx 15$ mW at 2.2 GHz.

jumps between two bistable states occur at ω_{up} and ω_{down} where $da/d\omega = \pm\infty$ as indicated by the arrows in Fig. 1(d).

The focus of this Rapid Communication is to highlight the effects of a nonlinear friction force such as a term proportional to $\dot{x}^3$ in $g(x,\dot{x})$. We demonstrate that such a nonlinear dissipation has profound impact on nonlinear dynamics, which we measure precisely in ferromagnetic metals using spin dynamos.[12]

Two sets of spin dynamos are used in this work. As shown in Fig. 1(f), sample I from the 1st-generation spin dynamos[12] has two identical Py microstrips (with width $W=20$ μm and thickness $d=130$ nm) deposited in both slots between the conductors of a ground-signal-ground (G-S-G) coplanar waveguide (CPW). Such a lateral coupling structure yields a weak in-plane h field but induces a strong rf current, which enhances the sensitivity of electrical detection of linear FMR.[12,14] Sample II as shown in Fig. 1(g) is one of the second generation spin dynamos. Here the Py microstrip ($W=5$ μm, $d=100$ nm) is embedded under the shorted conductor of the S and G strips and it is isolated from the CPW by a 200 nm SiO_2 layer to enable electrical detection of FMR. Such vertical coupling architecture boosts the in-plane h field by two orders of magnitude for nonlinear measurements.

We first characterize the properties of the devices. Anisotropic magnetoresistance (AMR) is measured under a perpendicular magnetic field H as depicted in Fig. 2(a) for sample I. Applying microwaves induces magnetization precession via FMR, which causes a resistance change by a factor of 10^{-6}. Such a small photoresistance[15] is sensitively detected by using lock-in techniques, where the output microwave power P is modulated by 100% at 8.3 kHz. Typical data measured at $\omega/2\pi=2.2$ GHz with $P=3$ and 23 dBm are plotted in the inset, showing linear and nonlinear FMR, respectively. Fitting the linear FMR to the Kittel formula of $\omega=\gamma(H-M_0)$ and Eq. (1), for sample I(II) we determine $\mu_0 M_0=1.025(1.000)$ T, $\gamma/2\pi=28.6(29.2)$ μ_0GHz/T, $\alpha=0.005(0.009)$, and $\mu_0\Delta H_i=0.08(0.88)$ mT. The different values for the two samples are caused by their different fabrication procedures, which result in a slightly different composition and quality of the Py microstrips.

The FMR shifts toward lower H field with increased power P, as shown in Fig. 2(b) with the mapping of the photoresistance measured at $\omega/2\pi=2.2$ GHz. This behavior reflects the nonlinear magnetization dynamics: by increasing P, the cone angle θ of the magnetization precession increases, so that the perpendicular magnetization reduces[16] from the saturation value M_0 to $M_0(1-\theta^2/2)$, which shifts the resonant field from $H_0=\omega/\gamma+M_0$ to $H_R=H_0-M_0\theta^2/2$. We find that the measured low power resonance field can be fitted by using $\theta^2=1.7\times10^{-4}P(\text{mW})$, while the high power data indicate a very different relation of $\theta^2=1.0\times10^{-3}P^{1/3}$. The crossing point of the fitted H_R curves gives a rough estimate of a threshold power of $P_{th}\approx15$ mW.

The power dependence of θ^2 can be determined independently from the photoresistance ΔR, since our previous study[15] shows that $\Delta R \propto \theta^2$. As plotted in Fig. 2(c), ΔR measured at 2.2 GHz confirms that $\theta^2 \propto P$ and $\theta^2 \propto P^{1/3}$ for $P \ll P_{th}$ and $P \gg P_{th}$, respectively. Further, it is found that P_{th} is frequency dependent. The existence of P_{th} separating two power regimes is an important feature of nonlinear dynamics,[3,17] which we study more precisely via photovoltage measurements.

In contrast to the photoresistance caused by a dynamic AMR effect[15] which is proportional to θ^2, the photovoltage is induced by the spin-rectification effect[12] which is proportional to θ in the first order. Hence this technique has very high sensitivity[14] and enables electrical detection of foldover effect of FMR in a ferromagnetic metal, as plotted in Figs. 3(a) and 3(b) for samples I and II, respectively. For comparison, linear FMR measured at lower power is plotted, where the side peaks are magnetostatic spin waves.[14] From the up- and down-sweep traces of the foldover FMR, we determine H_{up} and H_{down}, and plot their power dependence in Figs. 3(c) and 3(d) for sample I and II, respectively.

To elucidate the physics of the nonlinear magnetization dynamics, we solve the nonlinear oscillator equation by taking into account the effect of a nonlinear restoring force and nonlinear dissipation to the lowest (cubic) order on the same footing, which induce, respectively, amplitude-dependent resonance shifts and broadening in the general form of the solution. By writing the solution in the ansatz of the cone angle θ for magnetization precession to include specific physical parameters for magnetization dynamics, we obtain

$$\theta^2 = \frac{h^2}{(H - H_0 + M_0\theta^2/2)^2 + (\Delta H_0 + \beta M_0\theta^2)^2}, \qquad (3)$$

where the rf magnetic field h that drives the FMR is related to the microwave power P via the relation $h=S\sqrt{P}$. The sen-

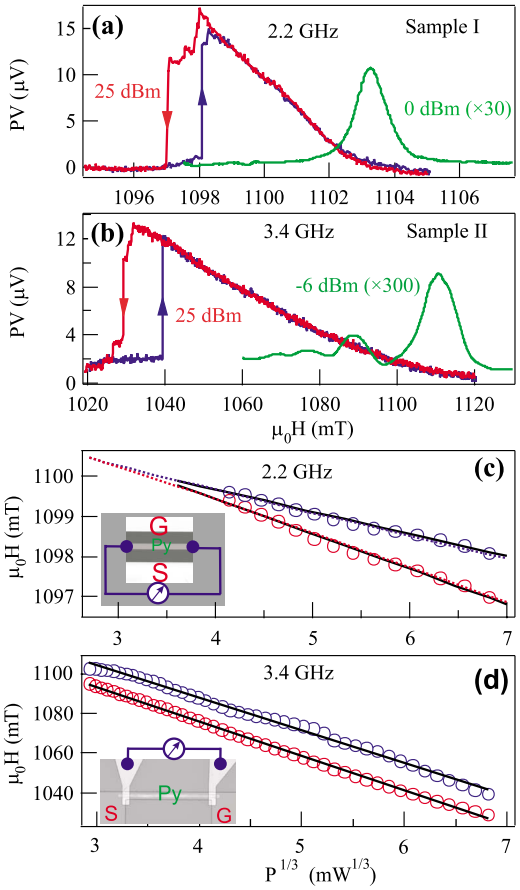

FIG. 3. (Color online) Linear and foldover FMR detected by photovoltages measured on (a) sample I and (b) sample II. Power dependence of H_{up} and H_{down} (circles) determined from the foldover FMR of (c) sample I and (d) sample II. Solid lines are theoretical fits. Dotted lines in (c) are calculated via Eq. (3) by using the fitted values of S and β.

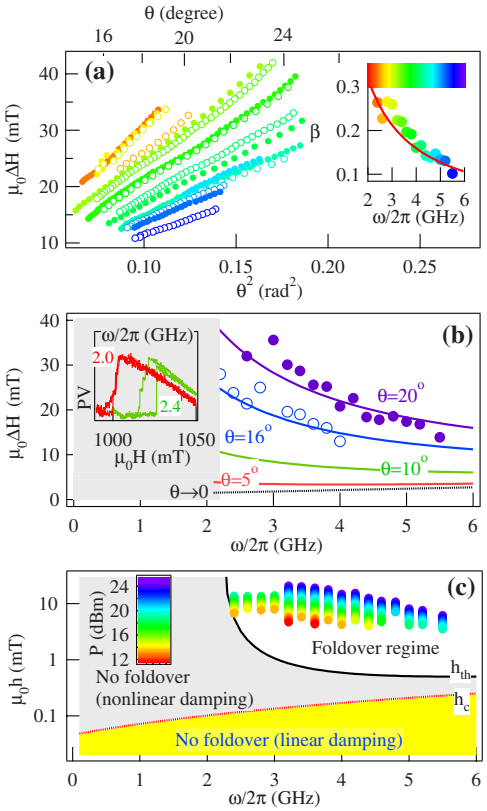

FIG. 4. (Color online) (a) Cone-angle (power) dependence of ΔH measured at different frequencies. Inset shows the measured (circles) ω dependence of β and the empirical relation (solid curve) of $\beta=4.0/\omega$. (b) ω dependence of ΔH (solid curves) and ΔH_0 (dotted line) calculated at different cone angles by using Eqs. (2) and (1), respectively. Circles show ΔH measured from foldover FMR. Inset shows two FMR spectra measured below and above 2.2 GHz. (c) ω dependence of Anderson-Suhl critical field h_c (dotted curve) and the threshold field h_{th} (solid curve). Note the suppressed region for detecting foldover FMR due to nonlinear damping, as confirmed by the photovoltage measurements (symbols).

sitivity parameter S depends on the sample design and microwave frequency ω.

In the limit of $h \to 0$, Eq. (3) reduces to the linear FMR with a Lorentzian lineshape, as shown in Fig. 1. Solving Eq. (3) analytically, we obtain the threshold field

$$h_{th}^2 = \frac{16\sqrt{3}(1+4\beta^2)}{9(1-2\sqrt{3}\beta)^3}\frac{\Delta H_0^3}{M_0}. \quad (4)$$

Foldover FMR appears at $h > h_{th}$. Note that if nonlinear damping is neglected ($\beta \to 0$), Eq. (4) reproduces the Anderson-Suhl critical field[3] given by $h_c^2 = 3.08\Delta H_0^3/M_0$. With nonlinear damping, the two abrupt jumps occur at the fields of $H_{up} \approx H_0 - (3/2)S^{2/3}(M_0 P)^{1/3}$ and $H_{down} \approx H_0 - S^2 M_0 P/2\Delta H^2 \approx H_0 - (1/2)(1+3\beta^2)(S/\beta)^{2/3}(M_0 P)^{1/3}$. Note that H_{up} is independent of damping and allows the calibration of the sensitivity parameter S, while H_{down} depends on ΔH defined by Eq. (2), which enables precise measurement of the nonlinear damping parameter β.

Fitting first H_{up} using this model, we obtain $S = 7.3 \times 10^{-3}$ mT/$\sqrt{\text{mW}}$ for sample I at 2.2 GHz, and $S = 1.2$ mT/$\sqrt{\text{mW}}$ for sample II at 3.4 GHz. As expected, the RF magnetic field in the 2nd generation spin dynamos is significantly boosted. By fixing the value of S, the measured power dependence of H_{down} can be fitted by using β as the only adjustable parameter. The fitting procedure works remarkably well as shown in Figs. 3(c) and 3(d). We obtain the nonlinear damping constant $\beta = 0.10 \pm 0.01$ and 0.22 ± 0.03, for sample I at 2.2 GHz and sample II at 3.4 GHz, respectively. The corresponding threshold powers (cone angles) are $P_{th} = 19.6$ mW ($\theta_{th} = 2.3°$) and 2.2 mW (8.5°).

Note, this model also explains the photoresistance shown in Fig. 2. Using Eq. (3), it is straightforward to prove that the cone angle at the resonance field H_R is given by $\theta_{\max} = S\sqrt{P}/\Delta H$. It follows from Eq. (2) that $\theta_{\max}^2 \approx (S/\Delta H_0)^2 P$ for $P \ll P_{th}$, and $\theta_{\max}^2 \approx (S/\beta M_0)^{2/3} P^{1/3}$ for $P \gg P_{th}$. This explains the empirical relations of $\theta(P)$, which we used in Fig. 2.

It is remarkable that such a simple phenomenological model, which involves only two parameters S and β, explains so well both photoresistance and photovoltage experiments, where the power dependence of four quantities (H_R, $\theta_{\max}$, H_{up}, and H_{down}) can be independently measured. We now use this model to highlight distinct characteristics of nonlinear magnetization damping.

Figure 4(a) shows the θ dependence of ΔH measured on sample II at different frequencies, where ΔH is determined from the measured value of H_{down}, and $\theta^2 \approx (S/\beta M_0)^{2/3} P^{1/3}(1-3\beta^2)$ is the corresponding cone angle at the field H_{down}. Following Eq. (2), the data indicate that β is larger at lower frequencies. In the inset of Fig. 4(a), the measured ω dependence of β is plotted and an empirical relation $\beta=4.0/\omega$(GHz) is found for $\omega/2\pi>2.2$ GHz. The revealed reduction of nonlinear dissipation at high frequencies is in marked contrast with the ferromagnetic dissipation described by Eq. (1). To demonstrate the dramatic difference, in Fig. 4(b) we plot $\Delta H(\omega)$ calculated at different cone angles by using Eq. (2) and the empirical relation $\beta=4.0/\omega$. Comparing ΔH to ΔH_0, it is clear that the region of validity of Eq. (1) is confined to very small cone angles.

The measured ΔH, plotted by circles in Fig. 4(b), leads to a more subtle and interesting aspect of nonlinear magnetization dynamics. As expected, the foldover FMR is detected only at large cone angles. But surprisingly, the effect is only observed at high frequencies. Bistability in sample II vanishes at $\omega/2\pi<2.2$ GHz, as shown in the inset of Fig. 4(b) with two spectra measured at $P=100$ mW below and above this threshold frequency. Similar effect is found in other samples but with different threshold frequencies. This result reveals the distinctive feature induced by nonlinear magnetization damping, which is illustrated by Fig. 4(c). If nonlinear damping is neglected ($\beta=0$), the threshold RF field h_{th} reduces to the Anderson-Suhl critical field[3] h_c, which is plotted in Fig. 4(c) as the dotted curve. Bistable states and foldover would be expected to appear in the region of $h>h_c$ in such a "phase diagram" of dynamic response. However, due to nonlinear damping, the region of bistability is significantly suppressed, particularly at low frequencies. The h_{th} calculated by employing the empirical relation $\beta=4.0/\omega$ is plotted in Fig. 4(c) by the solid curve. Indeed, foldover and bistabilty is only detected (solid circle) in the reduced region $h>h_{th}$. This resolves the long-standing mystery.

Finally, for completeness, we also solved the Landau-Lifshitz-Gilbert (LLG) equation to compare with the oscillator model. As expected,[3] the nonlinear restoring force is induced by the change of surface demagnetization field due to the precessions at large cone angles. However, the LLG equation for a uniform magnetization predicts a motion narrowing for large cone-angle precessions, which is in stark contrast to the nonlinear damping term revealed in the oscillator model. Therefore, the precisely measured enhanced damping, which is pivotal in revising both Eq. (1) and the Anderson-Suhl critical field, indicates intrinsic nonlinear damping in ferromagnetic metals due to magnon scattering effects, which is a subject of significant theoretical interest.[10] We conclude that spin dynamo devices, in combination with sensitive electrical probing techniques and the instructive analytic method, pave a way to study nonlinear dynamics in conducting ferromagnetic metals and ferromagnetic semiconductors, which is critical for the development of technologies such as nonlinear magnetic switching,[5] spin-torque transfer devices,[6,18] and domain-wall engineering.[19,20]

We thank Peter Loly and Xiao-Long Fan for helpful discussions. This work has been funded by NSERC, CFI, and URGP.

*hu@physics.umanitoba.ca; http://www.physics.umanitoba.ca/~hu

[1] G. Roger, *Galileo's Pendulum, From the Rhythm of Time to the Making of Matter*, 3rd ed. (Harvard University Press, Newton, 2004).

[2] L. D. Landau and E. M. Lifshitz, *Mechanics*, 3rd ed. (Pergamon Press, Oxford, 1976).

[3] P. W. Anderson and H. Suhl, Phys. Rev. **100**, 1788 (1955).

[4] G. Bertotti, I. D. Mayergoyz, and C. Serpico, Phys. Rev. Lett. **87**, 217203 (2001).

[5] C. Thirion, W. Wernsdorfer, and D. Mailly, Nature Mater. **2**, 524 (2003).

[6] S. I. Kiselev, J. C. Sankey, I. N. Krivorotov, N. C. Emley, R. J. Schoelkopf, R. A. Buhrman, and D. C. Ralph, Nature (London) **425**, 380 (2003).

[7] M. Sparks, *Ferromagnetic-Relaxation Theory* (McGraw-Hill, New York, 1964).

[8] T. L. Gilbert, Ph.D. thesis, Illinois Institute of Technology, 1956; IEEE Trans. Magn. **40**, 3443 (2004).

[9] B. Heinrich, J. F. Cochran, and R. Hasegawa, J. Appl. Phys. **57**, 3690 (1985).

[10] A. Yu. Dobin and R. H. Victora, Phys. Rev. Lett. **90**, 167203 (2003).

[11] V. Tiberkevich and A. N. Slavin, Phys. Rev. B **75**, 014440 (2007).

[12] Y. S. Gui, N. Mecking, X. Zhou, G. Williams, and C.-M. Hu, Phys. Rev. Lett. **98**, 107602 (2007).

[13] Foldover FMR was observed only in a ferromagnetic insultor yttrium iron garnet. See M. T. Weiss, Phys. Rev. Lett. **1**, 239 (1958).

[14] Y. S. Gui, N. Mecking, and C.-M. Hu, Phys. Rev. Lett. **98**, 217603 (2007).

[15] N. Mecking, Y. S. Gui, and C.-M. Hu, Phys. Rev. B **76**, 224430 (2007); Y. S. Gui, N. Mecking, A. Wirthmann, L. H. Bai, and C.-M. Hu, Appl. Phys. Lett. **91**, 082503 (2007).

[16] Microwave heating may also induce shift in FMR. We monitor this effect carefully by using the bolometric effect (Ref. 15). The dissipated microwave energy at 22 dBm output power increases the temperature of the sample by a few kelvins. The thermal induced change of the perpendicular magnetization is about a few tenth mT, which is at least an order of magnitude smaller than the intrinsic nonlinear effect observed here.

[17] T. Gerrits, P. Krivosik, M. L. Schneider, C. E. Patton, and T. J. Silva, Phys. Rev. Lett. **98**, 207602 (2007); H. M. Olson, P. Krivosik, K. Srinivasan, and C. E. Patton, J. Appl. Phys. **102**, 023904 (2007).

[18] J.-V. Kim, V. Tiberkevich, and A. N. Slavin, Phys. Rev. Lett. **100**, 017207 (2008).

[19] L. Thomas, M. Hayashi, X. Jiang, R. Moriya, C. Rettner, and S. S. P. Parkin, Nature (London) **443**, 197 (2006).

[20] M. Yamanouchi, J. Ieda, F. Matsukura, S. E. Barnes, S. Maekawa, and H. Ohno, Science **317**, 1726 (2007).